Journal of Biomaterials
2023; 7(1): 1-7
http://www.sciencepublishinggroup.com/j/jb
doi: 10.11648/j.jb.20230701.11
ISSN: 2640-2602 (Print); ISSN: 2640-2629 (Online)

Investigation of the Effect of Silicon Concentration on Biocompatibility and Bioactivity of Spray Pyrolyzed Bioactive Glass

Tsion Chuni Aklilu[1], Bethelhem Gashaw Ewnete[1], Megersa Aboneh Mekuria[2], Aster Aberra Tessema[3], Filimon Hadish[1], Fetene Fufa Bakare[1, 4, *]

[1]Department of Materials Science and Engineering, Adama Science and Technology University, Adama, Ethiopia

[2]Animal Biotechnology Directorate, Bio and Emerging Institute Technology, Addis Ababa, Ethiopia

[3]Department of Chemistry, Salale University, Oromia, Ethiopia

[4]Department of Advanced Materials Science and Engineering Center of Excellence, Adama Science and Technology University, Adama, Ethiopia

Email address:

hayu.fufa@gmail.com (Fetene Fufa Bakare)

[*]Corresponding author

To cite this article:

Tsion Chuni Aklilu, Bethelhem Gashaw Ewnete, Megersa Aboneh Mekuria, Aster Aberra Tessema, Filimon Hadish et al. (2023). Investigation of the Effect of Silicon Concentration on Biocompatibility and Bioactivity of Spray Pyrolyzed Bioactive Glass. *Journal of Biomaterials*, *7*(1), 1-7. https://doi.org/10.11648/j.jb.20230701.11

Received: October 26, 2023; **Accepted**: November 22, 2023; **Published**: December 6, 2023

Abstract: Bioactive glass is a prominent biomaterial that can bind with both soft and hard tissues when in contact with body fluid. This study aims to find out how silicon concentration affects the cytotoxicity and bioactivity of bioactive glass. The 58S, 68S, and 76S BG particles were synthesized using a spray pyrolysis method. XRD, SEM, FTIR, and BET were used to examine the phase composition, morphology, chemical identity, and specific surface area of BG powders. The ability of the specimens to generate apatite on their surface after being soaked in the simulated body fluid (SBF) was determined using an in vitro test to measure their bioactivity. To evaluate the bioactivity of the BG powders, the in vitro apatite formation was investigated using XRD, FTIR, and SEM. Also, an in vitro cytotoxicity test was done using (MTT assay). A cell-growing environment was used to evaluate the in vitro cytotoxicity test based on different extraction concentrations of glass particles. The experimental results suggested that as silicon concentration in the BG increased, cell viability increased whereas bioactivity was reduced. Finally, the correlation between silicon content and cell viability and bioactivity was explored.

Keywords: Bioactive Glass, Bioactivity, Cytotoxicity, Silicon Concentration, Spray Pyrolysis

1. Introduction

Due to trauma, aging, illness, nutritional inefficiency, and other factors, loss of bone function has become frequent occurrence [1]. Since bone loss often has serious functional and aesthetic consequences, it was essential to discover ways for bone tissue regeneration [2]. Several exploring of materials were done for the musculoskeletal disease and traumas. Biomaterial that chemically attach to bone has been made possible by Larry Hench's discovery of 45S5 bioglass which is the first bioactive ceramic [3]. Bioactive glass is a material with specific biological response at the interface and have potential for regenerating bone tissue [4]. Bioactive glass is more suitable to be utilized as a biomaterial due to its bioactivity, biocompatibility (nontoxicity), and biodegradability [5-7]. The bioactivity has been investigated in vitro when BG interacts with biological fluids and in vivo when it interacts with bone tissue [3]. The inorganic component of human bone, crystalline hydroxycarbonate apatite (HCA), is formed when simulated bodily fluid (SBF) is introduced to BGs, and this process has been used to illustrate BGs in vitro bioactivity [8, 9]. The emergence of a silica-rich gel layer and subsequent precipitation of a calcium phosphate layer of bioactive materials occurs as a result of

the partial dissolution of the bioactive glass surface [10]. As a result, silicate-based glasses have demonstrated the ability to bond to living tissue, particularly bone [11].

Silica concentration in the bioactive glass is crucial for the bioactivity and biocompatibility [12]. In silica-based bioactive glasses, an open network structure containing the SiOx tetrahedron is formed. K^{+1}, Ca^{+2}, and Na^{+1} are examples of alkali and/or alkali-earth cations that can fit with in the open structure [13]. These cations act as network modifiers by rupturing some Si-O-Si bonds, disrupting the continuity of the glassy structure, and producing non-bridging oxygen connections [14]. This non-bridging link within the glassy network is necessary for greater ion exchange, silica dissolution, and the development of a silica-rich layer on the surface, which are all important steps in the bioactivity process [10].

There are several BG powder synthesis methods such as melt-quench, sol-gel, and spray pyrolysis (SP). Bioglass material produced by the melting method is simple and suitable for mass production [15]. But, since mechanical milling is used to produce glass powders, it is difficult to produce finer particles and nanostructured materials [16]. In addition, it was fired at a very high temperature (above 1300°C), so they had dense structure and small specific surface area, which limits their properties [17]. The other technique is the sol-gel technique, a flexible procedure with low processing temperatures and chemical versatility [18]. Unfortunately, the entire procedure is batch production, requires many days and is challenging to morphological control [19, 20]. Instead, an SP technique provides continuous processing, a fast synthesis time, and a low synthesis temperature which is utilized to control the morphology of the particles [21, 22].

During the in vitro bioactivity estimation in simulated body fluid (SBF) for SiO_2-P_2O_5-CaO glass, the release of calcium ions (Ca^{2+}) from bioactive glasses may increase the degree of super saturation of the SBF solution and favors the nucleation of apatite onto the silica gel layer that was initially formed at the glass surface [23]. Nevertheless, Shinichi Maeno et al. demonstrated that osteoblast viability, proliferation, and differentiation in monolayer and 3D culture were influenced by calcium ion concentration [24]. Since alkali elements like Ca fit in the open structure of SiO_2 tetrahedron, its concentration varies with SiO_2. For lower Silica concentration in BG would enhance the release of more Ca and increase pH [25]. As a result, the cell viability decreases with the pH increase [25]. The higher pH can make stronger osmotic pressure which will make cells shrink and die [26]. Thus, we used glass compositions of 58S, 68S, and 76S BG powders by SP method for investigation of the impact of silica concentration on in-vitro cytotoxicity and in vitro bioactivity.

2. Materials and Methods

2.1. Synthesis

The BG powders in compositions of 58S (60mol% SiO_2, 36mol%CaO, and 4mol%P_2O_5), 68S (70mol% SiO_2, 26mol% CaO, and 4mol% P_2O_5), and 76S (80mol% SiO_2, 16mol% CaO, and 4mol% P_2O_5) were synthesized using spray pyrolysis method. Tetraethyl orthosilicate (TEOS, $Si(OC_2H_5)_4$, 99.9 wt%), calcium nitrate tetrahydrate (CN, $Ca(NO_3)_2$•$4H_2O$, 98.5 wt%), and triethyl phosphate (TEP, $(C_2H_5)_3PO_4$, 99.0%, Alfa Aesar, Heysham, UK) are the precursors used as Si, Ca, and P sources. TEOS, CN, and TEP were dissolved in 10g of 0.5M HCl and 360g of ethanol. A transparent solution was obtained after 6hr stirring of the precursor solution at room temperature. For the SP procedure, all precursor solutions were added to an ultrasonic atomizer (KT-100A, King Ultrasonic, New Taipei, Taiwan) that was set to operate at a frequency of 1.67 MHz. A tube furnace (D110, Dengyng, New Taipei, Taiwan) with three distinct heating zones was used to place the atomized droplets. Each zone's temperature was set to 250°C for preheating, 550°C for calcination, and 300°C for cooling. The surface of the powders produced was charged at the furnace's exit with a high voltage of 16 kV. An earthed stainless steel electrostatic collector was used to neutralize and condense the charged particles.

2.2. Characterization

XRD (D2 Phaser, Bruker, Karlsruhe, Germany) was used to obtain details of phase composition. A field-emission scanning electron microscope (JSM-6500F, JEOL, Tokyo, Japan) was used for analyzing the surface morphologies of BG powders. A constant-volume adsorption system was used to measure the specific surface areas of several BG powders at -196°C (Novatouch LX2, Quantachrome Instruments, Boynton Beach, Florida, USA). Before the BET measurements, the powders were degassed at 150°C for 3 hours. Moreover, Kokubo's simulated bodily fluid (SBF) test solution has previously been utilized for in vitro bioactivity studies [27]. All BG specimens were soaked in simulated body fluid (SBF), which has an ionic content comparable to that of human plasma, to test the in vitro bioactivity of all BGs. Each specimen was then submerged in SBF and submerged in water that was kept at a constant 37°C for 6 hours. The specimens were rinsed with acetone and deionized water following the removal of SBF, and then they were dried in an oven overnight. SEM, XRD, and FTIR analyses were used in the bioactivity test to examine the development of hydroxyapatite (HA) layers. Finally, 3-(4,5-dimethylthiazol-2-yl)-2,5-diphenyltetrazolium bromide was used for an in vitro cytotoxicity investigation (MTT assay). A cell-growing environment was used to evaluate the in vitro cytotoxicity test based on different extraction concentrations of glass particles [25].

3. Results

3.1. Morphology and Phase Composition

The XRD patterns of the 58S, 68S, and 76S BG specimens are shown in Figure 1. All BG specimens are amorphous,

with no crystalline peak, according to the XRD pattern, which reveals a broad peak between 20 and 30 degrees. Then, all compositions of BG specimens were successfully prepared with amorphous phase.

SEM micrographs of the 58S, 68S, and 76S BG powders are shown in Figure 2. The 58S BG powders' SEM micrographs revealed smooth particles with spherical shape, as depicted in Figure 2(a). Moreover, as can be seen in Figure 2(b), 68S BG particles have a surface morphology similar to that of 58S BG powders. Furthermore, in Figure 2(c), 76S BG powder showed smooth particles with spherical surface morphologies. The spray pyrolysis method's "one particle per drop" particle generation mechanism is what causes all spherical and smooth morphologies.

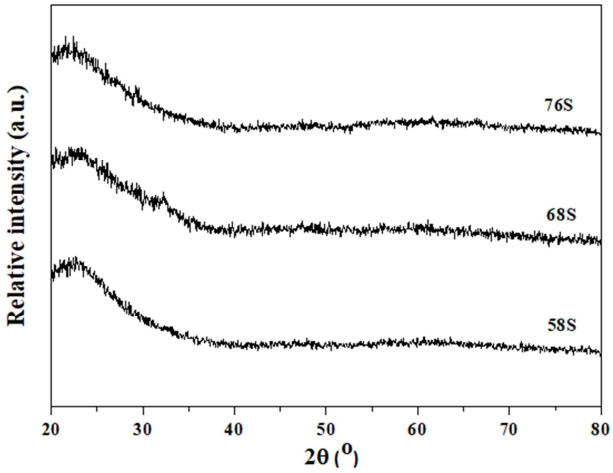

Figure 1. *XRD patterns of 58S, 68S, and 76S BG powders.*

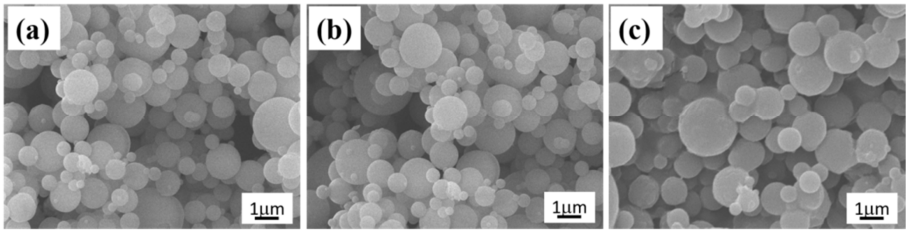

Figure 2. *SEM images of (a) 58S, (b) 68S and (c) 76S BG powders.*

3.2. In Vitro Cytotoxicity Analysis

The cell viability of 58S, 68S, and 76S BG powders is illustrated in Figure 3 as a function of extract concentration. Cell viability for 68S and 76S BG powders was greater than 70% at all extraction concentrations. For 58S BG powder 60% cell viability was obtained at 100% extraction. This indicates BG powders with higher silica concentration show higher cell viability or nontoxicity to the cell. However, smaller silica concentrations will result in lower cell viability.

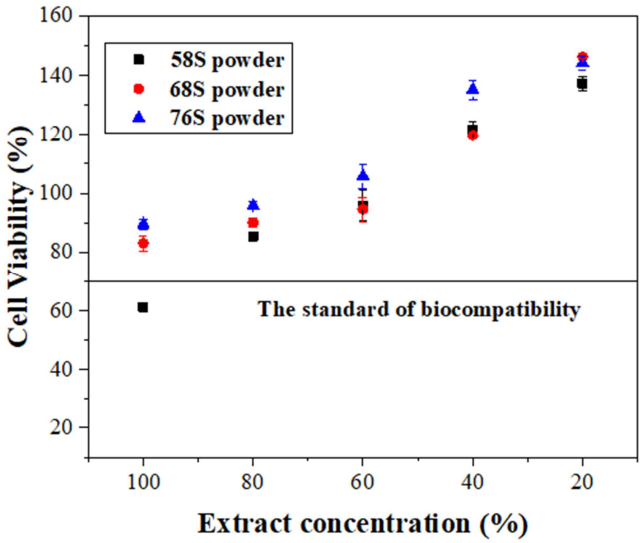

Figure 3. *Cell viability of 58S, 68S, and 76S BG powders with extract concentration.*

Figure 4 shows how the 58S, 68S, and 76S SiO_2 composition BGs are influencing the cell viability. For each SiO_2 concentration, the percentage of cell viability was assessed. Cell viability was detected as 60%, 80%, and 90% for the 58S, 68S, and 76S BG powders respectively. The cell viability of the 68S and 76S BG powders is greater than 70%, exceeding the standard nontoxic or cell viability limitations. As a result, cell viability was determined to be 76S > 68S > 58S, indicating that as silicon concentration in BG powders increased, so did cell viability.

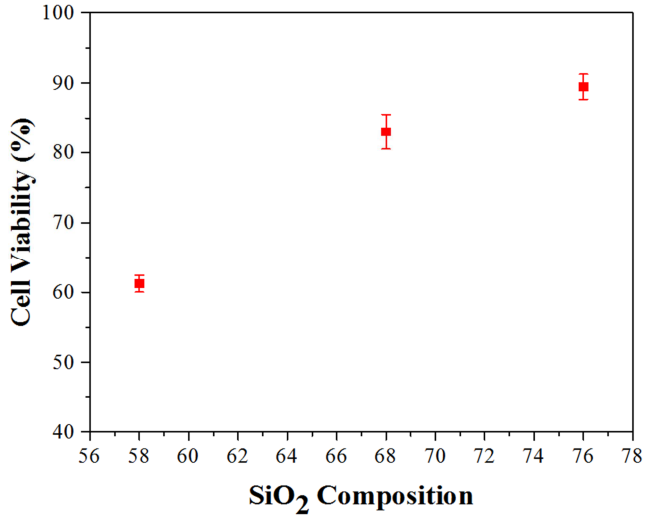

Figure 4. *Cell viability of 58S, 68S, and 76S BG powders with SiO_2 concentration.*

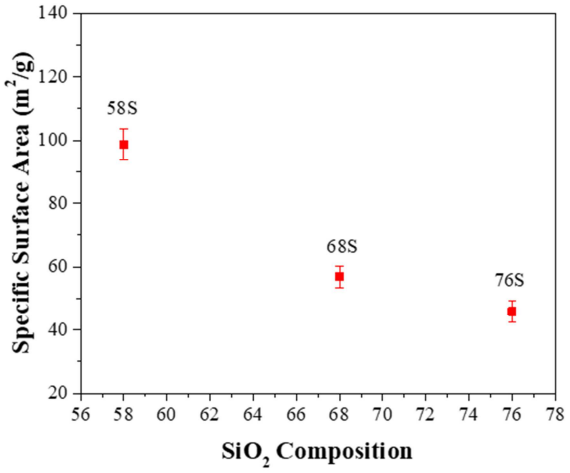

Figure 5. *The specific surface area of 58S, 68S, and 76S BG powders as a function of SiO_2 concentration.*

The relationship between the specific surface area and the SiO_2 composition of the 58S, 68S, and 76S BG powders is shown in Figure 5. The BET measurements, as seen in Figure 5, reveals that the 58S BG powder has a specific surface area of 98.7 + 4.9 m^2/g. Furthermore, 68S and 76S BG powders are 56.8 + 3.4, and 45.8 + 3.3 and m^2/g, respectively. The specific surface area of BG particles dropped as the silica concentration increased. The result revealed that smaller silica concentration induces higher specific surface area.

3.3. In Vitro Bioactivity

The SEM images of the 58S, 68S, and 76S BG specimens after 6 hours of immersion in the SBF solution are shown in Figure 6 for the in vitro bioactivity assays. The SEM image of the in vitro bioactivity formation results shows that smaller crystallites are growing on the surface of the BG particles.

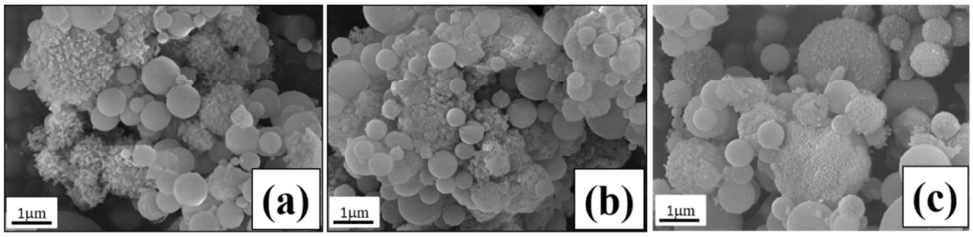

Figure 6. *SEM images of (a) 58S, (b) 68S and (c) 76S BG powders after immersed in SBF for 6hr.*

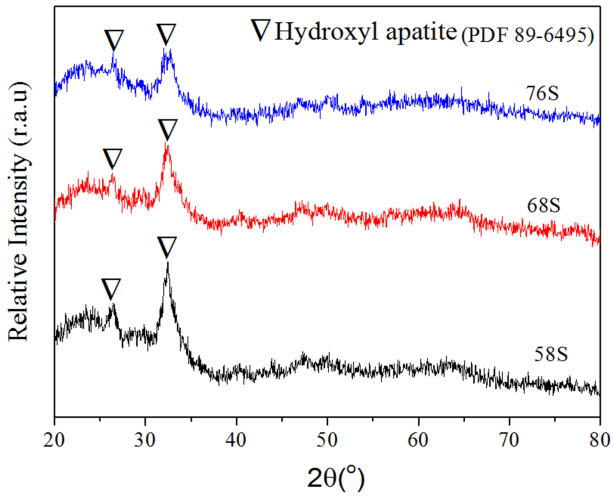

Figure 7. *XRD patterns of 58S, 68S, and 76S BG powders after being immersed in SBF for 6 hr.*

After being submerged in SBF for 6 hours, the XRD patterns of the 58S, 68S, and 76S BG powders are shown in Figure 7. All BG specimens showed diffraction peaks when compared to Figure 1. This shows that the hydroxyapatite (HA) layer formed after 6hr of immersion in SBF. Comparing the HA formation of the samples, 58S>68S>76S which indicates bioactivity increases with smaller Si concentration.

Then after, Figure 8 displays the FTIR spectra of the in-vitro bioactivity of the 58S, 68S, and 76S BG powders before and after being submerged in SBF for 6hr. Before being submerged in SBF, all specimens exhibit the Si-O-Si band, as seen in Figure 8a. As demonstrated in Figure 8b, all specimens display a fresh extra peak attributed to the P-O bending vibrations after soaking in SBF for 6 hours. Furthermore, the I_1/I_2 values for each specimen were determined so as to assess its bioactivity. While I2 refers to the intensity of Si-O-Si (Δ) bending vibration at 482 cm^{-1}, I_1 relates to the intensity of P-O (*) bending at 566 cm^{-1}. The I_1/I_2 results were computed as 0.57, 0.42, and 0.18 for 58S, 68S, and 76S BG powders, respectively, to determine each specimen's bioactivity. It can be concluded that BG specimens exhibit better bioactivity because of lower silica concentration since the higher I_1/I_2 value indicates better bioactivity.

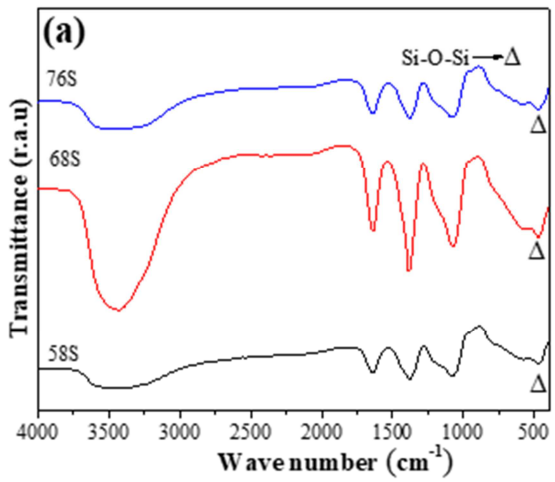

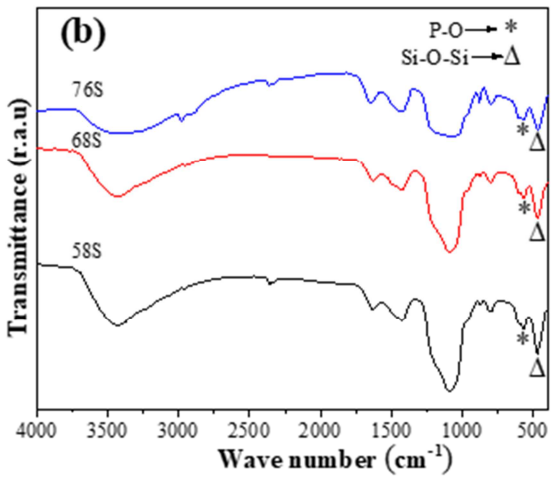

Figure 8. *FTIR spectra of 58S, 68S, and 76S BG powders (a) before and (b) after immersed in SBF for 6 hr.*

4. Discussion

Bioactivity and biocompatibility were influenced by silica concentration as shown on the obtained results. As silica concentration in BG increases, a structure with a stronger network is formed [28]. However, when the silica concentration decreased more non-bridging oxygen (NBO) will be formed. Its non-bridging bond promotes ion exchange, silica dissolution, and the development of a silica-rich layer on the surface, which is a crucial stage in the bioactivity process [10]. During in vitro bioactivity analysis in simulated bodily fluid (SBF), the release of calcium ions (Ca^{2+}) from bioactive glasses may increase the amount of super saturation of the SBF solution and trigger the nucleation of apatite onto the silica gel layer that was initially developed at the glass surface [26]. Figure 9 exhibits all spray-pyrolyzed BG powders as a function of SiO_2 content after 6 hours of immersion in SBF. It gives out bioactivity in the following order: 58S > 68S > 76S. A wide variety of physical and chemical reactions, including dissolution, diffusion, ionic exchange, and precipitation, are involved in the surface response process of BGs in SBF. Steps that result in the formation of the bioactive apatite layer are Ion release from the bioactive glass, the development of silanol groups (Si-OH) on the glass surface, the adsorption of calcium and phosphate ions on the glass surface, promoting the nucleation of amorphous calcium phosphate nanoclusters, and eventually the growth and crystallization of the calcium phosphate (apatite) layer [29]. For higher silica concentrations, dissolution of silica for ion exchange in the SBF is difficult because of its strong bond. The glass structure must have Si-O-NBO groups to facilitate ion exchange. The addition of network modifiers and lower silica content in the glass structure leads to the formation of non-bridging oxygen. Thus, BG with lower silica content exhibits better bioactivity. As the concentration of silica increased, cell viability was increased whereas bioactivity decreased as shown in Figure 9. Higher silica concentration in BG generates strong structures with reduced probability of NBO production. As a result, the BG and SBF solution's ability to exchange ions becomes less flexible, which reduces the glass's bioactivity and raises its cell viability by impeding the release of more Ca^{+2} ions into the solution. The formation of a Ca-P rich layer is facilitated by the enhanced migration of Ca^{+2} and PO_4^{3-} groups from the SBF to the surface, which also raises the pH of the SBF, in low SiO_2-containing BGs [26]. The viability, proliferation, and differentiation of osteoblasts in monolayer and 3D culture are affected by calcium ion concentration [24]. As a result, the cell viability decreases with the pH increase. The higher pH can make stronger osmotic pressure which will make cells shrink and die [26].

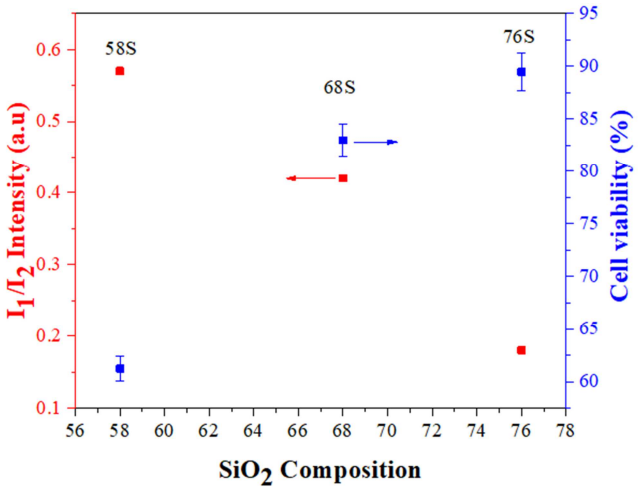

Figure 9. *Correlations of I_1/I_2 (bioactivity) and cell viability for 58S, 68S, and 76S BG powders.*

5. Conclusion

In this experiment 58S, 68S, and 76S BG powders were effectively synthesized with the spray pyrolysis technique. Generally, silica concentration has crucial role in the bioactivity and biocompatibility of BG. The composition and bonding configuration of silica-based BG has a great influence on in vitro bioactivity and biocompatibility. Surface morphologies were examined by SEM which reveals all BG particles have spherical morphology. According to a specific surface area analysis carried out using BET, BG particles with a high specific surface area can be formed at low SiO_2 concentrations. The in vitro bioactivity test was done by SEM, XRD, as well as FTIR analysis for compositions and amounts of crystal phase (HA) formation. As silica concentration increased, in vitro bioactivity and specific surface area BGs decreased. Also, cell viability increases with the concentration of silica in BG powders.

Data Availability

The data used to support the findings of this study are included in the article.

Authors Contributions

The study was designed by Fetene Fufa Bakare. The data analysis and interpretation was done by Tsion Chuni Aklilu, Bethelhem Gashaw Ewnete, Megersa Aboneh Mekuria, Aster Aberra Tessema and Fetene Fufa Bakare. The first draft of the manuscript was written by Tsion Chuni Aklilu. Review and editing, was done by Tsion Chuni, Fetene Fufa Bakare, Filimon Hadish, and Aster Aberra Tessema, all authors read and approved the final manuscript.

Acknowledgments

We acknowledge Adama Science and Technology University for materials support. The authors also acknowledge the National Taiwan University of Science and Technology for materials support and characterization of the samples, especially professor Shao-Ju Shih laboratory.

Conflicts of Interest

The authors declare that they have no conflict of interest.

References

[1] Anand A, Kundu B, Balla VK, Nandi SK. Synthesis and physico-chemical characterization of different mesoporous bioactive glass nanopowders: in-vitro SBF activity and cytotoxicity. Transactions of the Indian Ceramic Society. 2018; 77: 106-17.

[2] Skallevold HE, Rokaya D, Khurshid Z, Zafar MS. Bioactive glass applications in dentistry. International Journal of Molecular Sciences. 2019; 20: 5960.

[3] Hench LL. The story of Bioglass®. Journal of Materials Science: Materials in Medicine. 2006; 17: 967-78.

[4] Ansari M. Bone tissue regeneration: biology, strategies and interface studies. Progress in biomaterials. 2019; 8: 223-37.

[5] Bakare FF, Chou YJ, Huang YH, Tesfay AH, Moriga T, Shih SJ. Correlation of Morphology and In-Vitro Degradation Behavior of Spray Pyrolyzed Bioactive Glasses. Materials (Basel). 2019; 12.

[6] Lei B, Chen X, Koh Y-H. Effects of acidic catalysts on the microstructure and biological property of sol–gel bioactive glass microspheres. Journal of sol-gel science and technology. 2011; 58: 656-63.

[7] Hong B-J, Hsiao C-W, Bakare FF, Sun J-T, Shih S-J. Effect of Acetic Acid Concentration on Pore Structure for Mesoporous Bioactive Glass during Spray Pyrolysis. Materials (Basel). 2018; 11: 963.

[8] Hench LL, Polak JM. Third-generation biomedical materials. Science. 2002; 295: 1014-7.

[9] Deshmukh K, Kovářík T, Křenek T, Docheva D, Stich T, Pola J. Recent advances and future perspectives of sol–gel derived porous bioactive glasses: a review. RSC advances. 2020; 10: 33782-835.

[10] Serra J, Gonzalez P, Liste S, Chiussi S, Leon B, Pérez-Amor M, et al. Influence of the non-bridging oxygen groups on the bioactivity of silicate glasses. Journal of Materials science: Materials in medicine. 2002; 13: 1221-5.

[11] Karlsson KH, Fröberg K, Ringbom T. A structural approach to bone adhering of bioactive glasses. Journal of Non-Crystalline Solids. 1989; 112: 69-72.

[12] Hadush Tesfay A, Chou Y-J, Tan C-Y, Fufa Bakare F, Tsou N-T, Huang E-W, et al. Control of dopant distribution in yttrium-doped bioactive glass for selective internal radiotherapy applications using spray pyrolysis. Materials. 2019; 12: 986.

[13] Pouroutzidou GK, Liverani L, Theocharidou A, Tsamesidis I, Lazaridou M, Christodoulou E, et al. Synthesis and characterization of mesoporous mg-and sr-doped nanoparticles for moxifloxacin drug delivery in promising tissue engineering applications. International Journal of Molecular Sciences. 2021; 22: 577.

[14] Vernè E, Miola M, Renzi E. Synthesis and characterization of innovative silica-based bioactive glass doped with tellurium. 2019.

[15] Fiume E, Migneco C, Verné E, Baino F. Comparison between bioactive sol-gel and melt-derived glasses/glass-ceramics based on the multicomponent SiO_2–P_2O_5–CaO–MgO–Na_2O–K_2O system. Materials. 2020; 13: 540.

[16] Sarkar SK, Sadiasa A, Lee BT. Synthesis of a novel bioactive glass using the ultrasonic energy assisted hydrothermal method and their biocompatibility evaluation. Journal of Materials Research. 2014; 29: 1781-9.

[17] Montazerian M, Zanotto ED. A guided walk through Larry Hench's monumental discoveries. Journal of Materials Science. 2017; 52: 8695-732.

[18] Lei B, Chen X, Wang Y, Zhao N. Synthesis and in vitro bioactivity of novel mesoporous hollow bioactive glass microspheres. Materials Letters. 2009; 63: 1719-21.

[19] Sumida K, Liang K, Reboul J, Ibarra IA, Furukawa S, Falcaro P. Sol–gel processing of metal–organic frameworks. Chemistry of Materials. 2017; 29: 2626-45.

[20] Lei Q, Guo J, Noureddine A, Wang A, Wuttke S, Brinker CJ, et al. Sol–gel-based advanced porous silica materials for biomedical applications. Advanced Functional Materials. 2020; 30: 1909539.

[21] Molino G, Bari A, Baino F, Fiorilli S, Vitale-Brovarone C. Electrophoretic deposition of spray-dried Sr-containing mesoporous bioactive glass spheres on glass–ceramic scaffolds for bone tissue regeneration. Journal of Materials Science. 2017; 52: 9103-14.

[22] Chou Y-J, Hsiao C-W, Tsou N-T, Wu M-H, Shih S-J. Preparation and in vitro bioactivity of micron-sized bioactive glass particles using spray drying method. Applied Sciences. 2018; 9: 19.

[23] Hayakawa S, Tsuru K, Ohtsuki C, Osaka A. Mechanism of apatite formation on a sodium silicate glass in a simulated body fluid. Journal of the American Ceramic Society. 1999; 82: 2155-60.

[24] Maeno S, Niki Y, Matsumoto H, Morioka H, Yatabe T, Funayama A, et al. The effect of calcium ion concentration on osteoblast viability, proliferation and differentiation in monolayer and 3D culture. Biomaterials. 2005; 26: 4847-55.

[25] Chuni T, Dachasa K, Gochole F, Hunde T, Bakare FF. Effect of Morphology on the In Vitro Bioactivity and Biocompatibility of Spray Pyrolyzed Bioactive Glass. Advances in Materials Science and Engineering. 2023; 2023.

[26] Mehrabi T, Mesgar AS, Mohammadi Z. Bioactive glasses: a promising therapeutic ion release strategy for enhancing wound healing. ACS Biomaterials Science & Engineering. 2020; 6: 5399-430.

[27] Kokubo T, Shigematsu M, Nagashima Y, Tashiro M, Nakamura T, Yamamuro T, et al. Apatite-and wollastonite-containg glass-ceramics for prosthetic application. Bulletin of the Institute for Chemical Research, Kyoto University. 1982; 60: 260-8.

[28] Zhu H, Zheng K, Boccaccini AR. Multi-functional silica-based mesoporous materials for simultaneous delivery of biologically active ions and therapeutic biomolecules. Acta Biomaterialia. 2021; 129: 1-17.

[29] Hench LL. An introduction to bioceramics: World scientific; 1993.